Edisson Sávio de Góes Maciel
edissonsavio@yahoo.com.br
Rua Demócrito Cavalcanti, 152 - Afogados
50750-080 Recife, PE. Brazil

Comparison Among Structured First Order Algorithms in the Solution of the Euler Equations in Two-Dimensions

The present work studies upwind schemes applied to the solution of aeronautical and aerospace problems. The Harten, the Frink, Parikh and Pirzadeh, the Liou and Steffen and the Radespiel and Kroll algorithms, all first order accurate in space, are studied. The Euler equations in conservative form, employing a finite volume formulation and a structured spatial discretization, in the two-dimensional space, are solved. A time splitting method and a Runge-Kutta method of five stages are used to perform the time march of the numerical schemes. The steady state physical problems of the supersonic flow along a ramp and around a blunt body configuration are studied. All algorithms are accelerated to the steady state solution using a spatially variable time step. This technique has proved excellent gains in terms of convergence ratio as reported in Maciel. The results have demonstrated that the Liou and Steffen scheme has presented the most critical solutions, in both example-cases, in relation to the others schemes and a more accurate solution, in terms of the determination of the stagnation pressure in the blunt body case, than the Harten and the Radespiel and Kroll schemes. In the ramp problem, the Harten scheme predicts the best pressure distribution along the ramp wall in comparison with theoretical results. In the blunt body problem, the Liou and Steffen scheme presents the highest value of Cp at the configuration nose in relation to the other schemes. Values of c_L and c_D have been accurately predicted by all schemes, except by the Harten scheme.
***Keywords**: Harten scheme, Frink, Parikh and Pirzadeh scheme, Liou and Steffen scheme, Radespiel and Kroll scheme, Euler equations*

Introduction

Conventional non-upwind algorithms have been used extensively to solve a wide variety of problems (Kutler, 1975, and Steger, 1978). Conventional algorithms are somewhat unreliable in the sense that for every different problem (and sometimes, every different case in the same class of problems) artificial dissipation terms must be specially tuned and judicially chosen for convergence. Also, complex problems with shocks and steep compression and expansion gradients may defy solution altogether.

Upwind schemes are in general more robust but are also more involved in their derivation and application. Some upwind schemes that have been applied to the Euler equations are: Roe (1981), Harten (1983), Frink, Parikh and Pirzadeh (1991), Liou and Steffen (1993) and Radespiel and Kroll (1995). Some comments about these methods are reported below:

Roe (1981) presented a work that emphasized that several numerical schemes to the solution of the hyperbolic conservation equations were based on exploring the information obtained in the solution of a sequence of Riemann problems. It was verified that in the existent schemes the major part of this information was degraded and that only certain solution aspects were solved. It was demonstrated that the information could be preserved by the construction of a matrix with a certain "U property". After the construction of this matrix, its eigenvalues could be considered as wave velocities of the Riemann problem and the U_L-U_R projections over the matrix's eigenvectors are the jumps which occur between intermediate stages.

Harten (1983) developed a class of new finite difference schemes, explicit and with second order of spatial accuracy to calculation of weak solutions of the hyperbolic conservation laws. These schemes highly non-linear were obtained by the application of a first order non-oscillatory scheme to an appropriated modified flux function. The so derived second order schemes reached high resolution, while preserved the robustness property of the original non-oscillatory scheme.

Frink, Parikh and Pirzadeh (1991) proposed a new scheme, unstructured and upwind, to the solution of the Euler equations. They tested the precision and the utility of this scheme in the analysis of the inviscid flows around two airplane configurations: one of transport configuration, with turbines under the wings, and the other of high speed civil configuration. Tests were accomplished at subsonic and transonic Mach numbers with the transport airplane and at transonic and low supersonic Mach numbers with the civil airplane.

Liou and Steffen (1993) proposed a new flux vector splitting scheme. They declared that their scheme was simple and its accuracy was equivalent and, in some cases, better than the Roe (1981) scheme accuracy in the solutions of the Euler and the Navier-Stokes equations. The scheme was robust and converged solutions were obtained so fast as the Roe (1981) scheme. The authors proposed the approximated definition of an advection Mach number at the cell face, using its neighbor cell values via associated characteristic velocities. This interface Mach number was so used to determine the upwind extrapolation of the convective quantities.

Radespiel and Kroll (1995) emphasized that the Liou and Steffen (1993) scheme had its merits of low computational complexity and low numerical diffusion as compared to other methods. They also mentioned that the original method had several deficiencies. The method yielded local pressure oscillations in the shock wave proximities, adverse mesh and flow alignment problems. In the Radespiel and Kroll (1995) work, a hybrid flux vector splitting scheme, which alternated between the Liou and Steffen (1993) scheme and the van Leer (1982) scheme, in the shock wave regions, is proposed, assuring that resolution of strength shocks was clear and sharply defined.

In this work, the Harten (1983), the Frink, Parikh and Pirzadeh (1991), the Liou and Steffen (1993) and the Radespiel and Kroll (1995) schemes are implemented, on a finite volume context and using an upwind and structured spatial discretization, to solve the Euler equations in the two-dimensional space. The physical

Paper accepted June, 2007. Technical Editor: Amir Antônio M. de Oliveira Jr.

problems of the supersonic flow along a ramp and around a blunt body configuration are studied. The implemented schemes are first order accurate in space. A spatially variable time step is used to accelerate the algorithms to the steady state solution. This technique has proved excellent gains in terms of convergence ratio as reported in Maciel (2005). The results have demonstrated that the Liou and Steffen (1993) scheme has yielded the most realistic solutions than the others schemes. More studies, with other example-cases, are predicted by the author, as future works, aiming to better highlight the algorithm characteristics.

Nomenclature

Latin Symbols

a = speed of sound in fluid, m/s
CFL = "Courant-Friedrichs-Lewy" number
e = total energy of fluid per unity volume, J/m^3
E_e, F_e = inviscid flux vectors (or Euler flux vectors) in x and y direction, respectively
H = local enthalpy, J/Kg
p = static pressure of fluid, N/m^2
Q = vector of conserved variables
S = surface area, m^2
u, v= x and y components of the velocity vector q, m/s
V = volume of a given computational cell, m^3
x, y= x and y spatial positions in the Cartesian coordinate system, respectively, m

Greek Symbols

α = attack angle, degrees, or projection vectors
Δt = time step, s
γ = ratio of specific heats, adopted 1.4 to atmospheric mean
ψ = entropy function
ρ = fluid density, kg/m^3

Subscripts

e Euler
i, j computational indexes

Euler Equations

The fluid movement is described by the Euler equations, which express the conservation of mass, of linear momentum and of energy to an inviscid, heat non-conductor and compressible mean, in the absence of external forces. In the conservative and integral forms, these equations can be represented by:

$$\partial/\partial t \int_V Q dV + \int_S \left[(E_e)n_x + (F_e)n_y\right] dS = 0 \,, \tag{1}$$

with Q written to a Cartesian system, V is the cell volume, n_x and n_y are the components of the normal unity vector to the flux face, S is the flux area and E_e and F_e are the components of the convective flux vector. The vectors Q, E_e and F_e are represented by:

$$Q = \begin{Bmatrix} \rho \\ \rho u \\ \rho v \\ e \end{Bmatrix}, \quad E_e = \begin{Bmatrix} \rho u \\ \rho u^2 + p \\ \rho uv \\ (e+p)u \end{Bmatrix} \quad and \quad F_e = \begin{Bmatrix} \rho v \\ \rho uv \\ \rho v^2 + p \\ (e+p)v \end{Bmatrix}; \tag{2}$$

being ρ the fluid density; u and v the Cartesian components of the velocity vector in the x and y directions, respectively; e the total energy per unit volume of the fluid mean; and p is the static pressure of the fluid mean.

The Euler equations are nondimensionalized in relation to the freestream density, ρ_∞, and in relation to the freestream speed of sound, a_∞, to the studied problems. The matrix system of the Euler equations is closed with the state equation of a perfect gas $p = (\gamma - 1)\left[e - 0.5\rho(u^2 + v^2)\right]$, assuming the ideal gas hypothesis and γ is the ratio of specific heats. The total enthalpy is determined by $H = (e + p)/\rho$.

Harten (1983) Algorithm

The Harten (1983) algorithm, first order accurate in space, is specific by the determination of the numerical flux vector at *(i+½,j)* interface. Its extension to the *(i,j+½)* interface is straightforward, without additional complications.

The right and left cell volumes, as well the interface volume, necessary to coordinate change, following a finite volume formulation, which is equivalent to a generalized system, are defined by:

$$V_R = V_{i+1,j}\,, \quad V_L = V_{i,j} \quad \text{and} \quad V_{\text{int}} = 0.5(V_R + V_L)\,, \tag{3}$$

where "*R*" and "*L*" represent right and left, respectively. The cell volume is defined by:

$$V_{i,j} = 0.5\left|(x_{i,j} - x_{i+1,j})y_{i+1,j+1} + (x_{i+1,j} - x_{i+1,j+1})y_{i,j} + (x_{i+1,j+1} - x_{i,j})y_{i+1,j}\right| + 0.5\left|(x_{i,j} - x_{i+1,j+1})y_{i,j+1} + (x_{i+1,j+1} - x_{i,j+1})y_{i,j} + (x_{i,j+1} - x_{i,j})y_{i+1,j+1}\right|. \tag{4}$$

The area components at interface are defined by: $S_{x\_\text{int}} = s_x' S$ and $S_{y\_\text{int}} = s_y' S$, where s_x' and s_y' are defined as: $s_x' = s_x / S$ and $s_y' = s_y / S$, being $S = \left(s_x^2 + s_y^2\right)^{0.5}$. Expressions to s_x and s_y, which represent the S_x and S_y components always adopted in the positive orientation, are given in Tab. 1.

Table 1. Normalized values of s_x and s_y.

Surface	s_x	s_y
i,j-1/2	$-(y_{i+1,j} - y_{i,j})$	$(x_{i+1,j} - x_{i,j})$
i+1/2,j	$(y_{i+1,j+1} - y_{i+1,j})$	$(x_{i+1,j} - x_{i+1,j+1})$
i,j+1/2	$(y_{i,j+1} - y_{i+1,j+1})$	$(x_{i+1,j+1} - x_{i,j+1})$
i-1/2,j	$(y_{i,j+1} - y_{i,j})$	$-(x_{i,j+1} - x_{i,j})$

The calculated properties at the flux interface are obtained either by arithmetical average or by Roe (1981) average. In this work, the arithmetical average was used. The speed of sound at the interface is determined by $a_{\text{int}} = \sqrt{(\gamma - 1)\left[H_{\text{int}} - 0.5\left(u_{\text{int}}^2 + v_{\text{int}}^2\right)\right]}$, where H_{int}, u_{int} and v_{int} are the flux interface properties.

The jumps of the conserved variable, necessary to the construction of the Harten (1983) dissipation function, are detailed in Maciel (2006). The α vectors to the *(i+½,j)* interface are also found in Maciel (2006). The Harten (1983) dissipation function is constructed using the matrix:

$$R_{i+1/2,j}=\begin{bmatrix} 1 & 1 & 0 & 1 \\ u_{\text{int}}-h_x^{'}a_{\text{int}} & u_{\text{int}} & -h_y^{'} & u_{\text{int}}+h_x^{'}a_{\text{int}} \\ v_{\text{int}}-h_y^{'}a_{\text{int}} & v_{\text{int}} & h_x^{'} & v_{\text{int}}+h_y^{'}a_{\text{int}} \\ H_{\text{int}}-h_x^{'}u_{\text{int}}a_{\text{int}}-h_y^{'}v_{\text{int}}a_{\text{int}} & 0.5\left(u_{\text{int}}^2+v_{\text{int}}^2\right) & h_x^{'}v_{\text{int}}-h_y^{'}u_{\text{int}} & H_{\text{int}}+h_x^{'}u_{\text{int}}a_{\text{int}}+h_y^{'}v_{\text{int}}a_{\text{int}} \end{bmatrix}, \tag{5}$$

where $h_x^{'}$ and $h_y^{'}$ are metric terms also defined in Maciel (2006). The entropy condition, determined by the ψ function, is implemented according to Harten (1983):

$$\psi_l=\begin{cases} |Z_l|, & \text{if } |Z_l|\geq\delta_f \\ 0{,}5\left(Z_l^2+\delta_f^2\right)\Big/\delta_f, & \text{if } |Z_l|<\delta_f \end{cases} \quad \text{and } \upsilon_l=\Delta t\lambda_l=Z_l; \tag{6}$$

with "*l*" varying from 1 to 4 (two-dimensional space) and δ_f assuming values between 0.1 and 0.5, being 0.2 the recommended value by Harten (1983).

The Harten (1983) dissipation function is constructed by the following matrix-vector product:

$$\{D_{Harten}\}_{i+1/2,j}=[R]_{i+1/2,j}\left\{-\psi\alpha\Big/\Delta t_{i,j}\right\}_{i+1/2,j}. \tag{7}$$

The convective numerical flux vector to the *(i+½,j)* interface is described by:

$$F_{i+1/2,j}^{(l)}=\left(E_{\text{int}}^{(l)}h_x+F_{\text{int}}^{(l)}h_y\right)V_{\text{int}}+0.5D_{Harten}^{(l)}, \tag{8}$$

with:

$$E_{\text{int}}^{(l)}=0.5\left(E_R^{(l)}+E_L^{(l)}\right) \text{ and } F_{\text{int}}^{(l)}=0.5\left(F_R^{(l)}+F_L^{(l)}\right); \tag{9}$$

The time integration is performed using a time splitting method, first order accurate in time, which separates the time integration in two steps, each one associated with a particular spatial direction. Details of this implementation are found in Maciel (2006).

Frink, Parikh and Pirzadeh (1991) Algorithm

In this scheme, first order accurate in space, the numerical flux vector is calculated using the Roe (1981) flux difference splitting method. The flux which crosses each *(i+½,j)* cell face is calculated using the Roe formula:

$$F_{i+1/2,j}=1/2\left[F(Q_L)+F(Q_R)-\left|\tilde{A}\right|(Q_R-Q_L)\right]_{i+1/2,j}. \tag{10}$$

The $\tilde{A}$ matrix is determined by the evaluation of $A=\partial F/\partial Q$, with the flow properties obtained by Roe (1981) average. The dissipation function of the Roe numerical flux vector formula, can be rewritten in terms of three flux components, each one associated with a distinct eigenvalue:

$$D_{FPP}=\left|\Delta\tilde{F}_1\right|+\left|\Delta\tilde{F}_3\right|+\left|\Delta\tilde{F}_4\right|, \tag{11}$$

where:

$$\left|\Delta\tilde{F}_1\right|=\left|\tilde{U}\right|\left\{\left(\Delta\rho-\frac{\Delta p}{\tilde{a}^2}\right)\begin{bmatrix}1\\ \tilde{u}\\ \tilde{v}\\ \frac{\tilde{u}^2+\tilde{v}^2}{2}\end{bmatrix}+\tilde{\rho}\begin{bmatrix}0\\ \Delta u-n_x\Delta U\\ \Delta v-n_y\Delta U\\ \tilde{u}\Delta u+\tilde{v}\Delta v-\tilde{U}\Delta U\end{bmatrix}\right\}$$

$$\text{and } \left|\Delta\tilde{F}_{3,4}\right|=\left|\tilde{U}\pm\tilde{a}\right|\left(\frac{\Delta p\pm\tilde{\rho}\tilde{a}\Delta U}{2\tilde{a}^2}\right)\begin{bmatrix}1\\ \tilde{u}\pm n_x\tilde{a}\\ \tilde{v}\pm n_y\tilde{a}\\ \tilde{h}\pm\tilde{U}\tilde{a}\end{bmatrix}, \tag{12}$$

with $\tilde{U}=\tilde{u}n_x+\tilde{v}n_y$ and $\Delta U=n_x\Delta u+n_y\Delta v$. The convective numerical flux vector at the *(i+½,j)* interface is defined as:

$$F_{i+1/2,j}^{(l)}=\left(E_{\text{int}}^{(l)}S_{x_{i+1/2,j}}+F_{\text{int}}^{(l)}S_{y_{i+1/2,j}}\right)+0.5D_{FPP}^{(l)}S_{i+1/2,j}. \tag{13}$$

The time integration is performed using an explicit Runge-Kutta method of five stages, second order accurate, defined in general form as:

$$\begin{aligned} Q_{i,j}^{(0)}&=Q_{i,j}^{(n)} \\ Q_{i,j}^{(k)}&=Q_{i,j}^{(0)}-\alpha_k\,\Delta t_{i,j}\Big/V_{i,j}\times C\left(Q_{i,j}^{(k-1)}\right), \\ Q_{i,j}^{(n+1)}&=Q_{i,j}^{(k)} \end{aligned} \tag{14}$$

with k = 1,...,5; α_1 = 1/4, α_2 = 1/6, α_3 = 3/8, α_4 = 1/2 and α_5 = 1; and C is the discrete approximation of the flux integral which contains the contributions from the flux vectors at each interface.

Liou nd Steffen (1993) Algorithm

The approximation of the integral Equation (1) to a rectangular finite volume yields an ordinary differential equation system with respect to time:

$$V_{i,j}\,dQ_{i,j}/dt=-R_{i,j}, \tag{15}$$

with $R_{i,j}$ representing the neat flux (residual) of conservation of mass, of linear momentum and of energy in the $V_{i,j}$ volume. The residual is calculated as:

$$R_{i,j}=R_{i+1/2,j}-R_{i-1/2,j}+R_{i,j+1/2}-R_{i,j-1/2}, \tag{16}$$

with $R_{i+1/2,j}=R_{i+1/2,j}^{c}$, where "c" is related to the flow convective contribution.

The discrete convective flux calculated by the AUSM ("Advection Upstream Splitting Method") scheme can be interpreted as a sum of the Mach number weighted average of the left (L) and the right (R) states of the *(i+½,j)* cell face, between volumes *(i,j)* and *(i+1,j)*, and a dissipative scalar term, as shown in

Liou and Steffen (1993). Hence,

$$R_{i+1/2,j} = |S|_{i+1/2,j} \left(\begin{array}{l} \frac{1}{2} M_{i+1/2,j} \left(\begin{bmatrix} \rho a \\ \rho a u \\ \rho a v \\ \rho a H \end{bmatrix}_L + \begin{bmatrix} \rho a \\ \rho a u \\ \rho a v \\ \rho a H \end{bmatrix}_R \right) - \\ -\frac{1}{2} \phi_{i+1/2,j} \left(\begin{bmatrix} \rho a \\ \rho a u \\ \rho a v \\ \rho a H \end{bmatrix}_R - \begin{bmatrix} \rho a \\ \rho a u \\ \rho a v \\ \rho a H \end{bmatrix}_L \right) \end{array} \right) + \begin{bmatrix} 0 \\ S_x p \\ S_y p \\ 0 \end{bmatrix}_{i+1/2,j} , \quad (17)$$

The "*a*" quantity represents the speed of sound, defined as $a = \sqrt{\gamma p / \rho}$. $M_{i+½,j}$ defines the advective Mach number at the *(i+½,j)* face of the *(i,j)* cell, which is calculated according to Liou and Steffen (1993) as:

$$M_{i+1/2,j} = M_L^p + M_R^m , \quad (18)$$

where the $M^{p/m}$ separated Mach numbers are defined by Van Leer (1982) and can also be found in Maciel (2007). M_L and M_R represent the Mach numbers associated with the left and right states, respectively. The advection Mach number is defined by:

$$M = \frac{1}{|S|} \frac{(S_x u + S_y v)}{a} . \quad (19)$$

The pressure at *(i+½,j)* face of the *(i,j)* cell is calculated by a similar way:

$$p_{i+1/2,j} = p_L^p + p_R^m , \quad (20)$$

with $p^{p/m}$ indicating the pressure separation defined according to Van Leer (1982) and also found in Maciel (2007).

The definition of the ϕ dissipative term determines the particular formulation of the convective fluxes. The choice below corresponds to the Liou and Steffen (1993) scheme, according to Radespiel and Kroll (1995):

$$\phi_{i+1/2,j} = \phi^{LS}_{i+1/2,j} = |M_{i+1/2,j}| . \quad (21)$$

The time integration is performed by the time splitting method detailed in Maciel (2006). This scheme is first order accurate in space.

Radespiel and Kroll (1995) Algorithm

The Radespiel and Kroll (1995) scheme is described by the Eqs. (15) to (20). The next step is the determination of the ϕ dissipative term. A hybrid scheme is proposed by Radespiel and Kroll (1995), which combines the Van Leer (1982) scheme and the Liou and Steffen (1993) (AUSM) scheme. Hence,

$$\phi_{i+1/2,j} = (1-\omega)\phi^{VL}_{i+1/2,j} + \omega \phi^{LS}_{i+1/2,j} , \quad (22)$$

with:

$$\phi^{VL}_{i+1/2,j} = \begin{cases} |M_{i+1/2,j}|, & \text{if } |M_{i+1/2,j}| \geq 1; \\ |M_{i+1/2,j}| + \frac{1}{2}(M_R - 1)^2, & \text{if } 0 \leq M_{i+1/2,j} < 1; \\ |M_{i+1/2,j}| + \frac{1}{2}(M_L + 1)^2, & \text{if } -1 < M_{i+1/2,j} \leq 0; \end{cases} \quad (23)$$

$$\phi^{LS}_{i+1/2,j} = \begin{cases} |M_{i+1/2,j}|, & \text{if } |M_{i+1/2,j}| > \tilde{\delta} \\ \frac{(M_{i+1/2,j})^2 + \tilde{\delta}^2}{2\tilde{\delta}}, & \text{if } |M_{i+1/2,j}| \leq \tilde{\delta} \end{cases} , \quad (24)$$

where $\tilde{\delta}$ is a small parameter, $0 < \tilde{\delta} \leq 0.5$, and ω is a constant, $0 \leq \omega \leq 1$. In this work, the values used to $\tilde{\delta}$ and ω were: 0.2 and 0.5, respectively. The time integration follows the method described in Maciel (2006). This scheme is first order accurate in space.

Spatially Variable Time Step

The basic idea of this procedure consists in keeping constant the CFL number in all computational domain, allowing, hence, the use of appropriated time steps to each specific mesh region during the convergence process. Details of the present implementation can be found in Maciel (2002) and in Maciel (2006).

Initial and Boundary Conditions

Initial Condition

Values of freestream flow are adopted for all properties as initial condition, in the whole calculation domain, to the physical problems studied in this work (Jameson and Mavriplis, 1986, Maciel, 2002, and Maciel, 2006).

Boundary Conditions

The boundary conditions are basically of three types: solid wall, entrance and exit. These conditions are implemented in special cells named ghost cells.

(a) Wall condition: This condition imposes the flow tangency at the solid wall. This condition is satisfied considering the wall tangent velocity component of the ghost volume as equals to the respective velocity component of its real neighbor cell. At the same way, the wall normal velocity component of the ghost cell is equaled in value, but with opposite signal, to the respective velocity component of the real neighbor cell.

The pressure gradient normal to the wall is assumed be equal to zero, following an inviscid formulation. The same hypothesis is applied to the temperature gradient normal to the wall. The ghost volume density and pressure are extrapolated from the respective values of the real neighbor volume (zero order extrapolation), with these two conditions. The total energy is obtained by the state equation of a perfect gas.

(b) Entrance condition:

(b.1) Subsonic flow: Three properties are specified and one is extrapolated, based on analysis of information propagation along characteristic directions in the calculation domain (Maciel, 2002). The pressure was the extrapolated variable from the real neighbor volume, to the studied problems. Density and velocity components had their values determined by the freestream flow properties.

(b.2) Supersonic flow: All variables are fixed with freestream flow values, at the entrance boundary.

(c) Exit condition:

(c.1) Subsonic flow: Three properties are extrapolated and one is specified, based on analysis of information propagation along characteristic directions in the calculation domain (Maciel, 2002). In this case, the ghost volume's pressure is specified by its initial value. Density and velocity components are extrapolated.

(c.2) Supersonic flow: All variables are extrapolated from the interior domain.

Results

Tests were performed in a CELERON-1.2GHz and 128 Mbytes of RAM memory microcomputer. Converged results occurred to 4 orders of reduction of the maximum residual value. The value used to γ was 1.4. A zero attack angle was adopted for all problems studied in this work.

Ramp Physical Problem

An algebraic mesh of 61x100 points was used to this problem. This mesh is composed of 5,940 rectangular volumes and 6,100 nodes on a finite volume context. The ramp configuration and the respective employed mesh are shown in Figs. 1 and 2. It was adopted a freestream Mach number of 2.0 as initial condition, characterizing a supersonic flow.

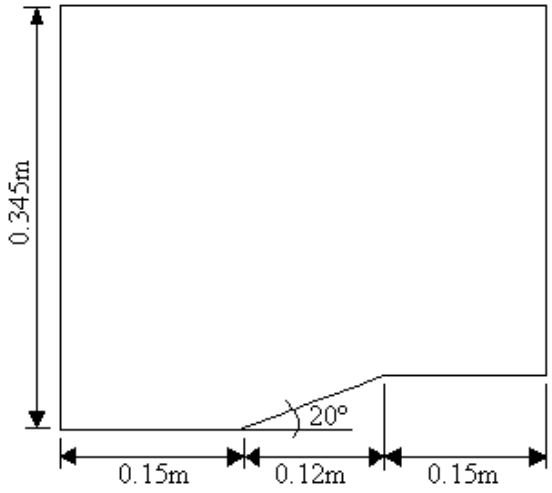

Figure 1. Ramp configuration.

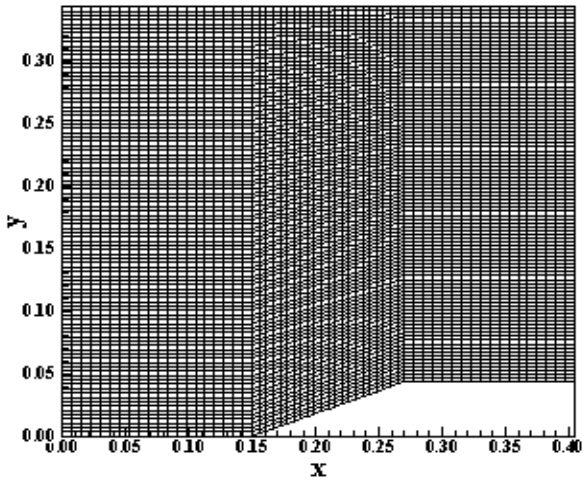

Figure 2. Ramp mesh.

Figures 3 to 6 show the density field obtained by the Harten (1983), the Frink, Parikh and Pirzadeh (1991), the Liou and Steffen (1993) and the Radespiel and Kroll (1995) schemes, respectively. The density field generated by the Liou and Steffen (1993) scheme is the densest at the shock region in relation to the others tested schemes.

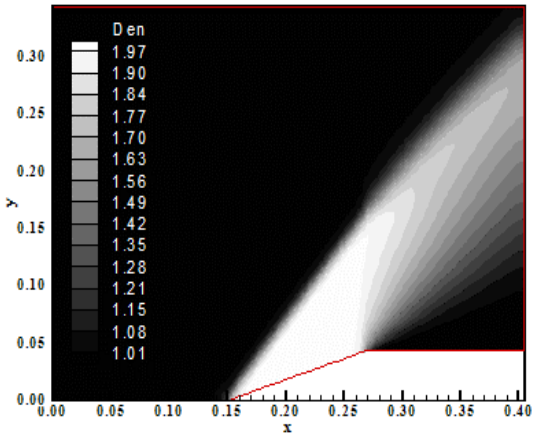

Figure 3. Density field (H/83).

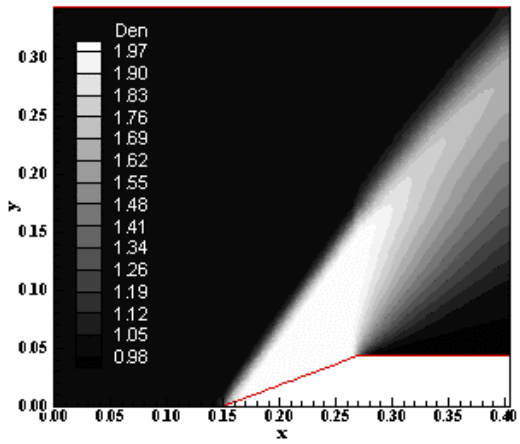

Figure 4. Density field (FPP/91).

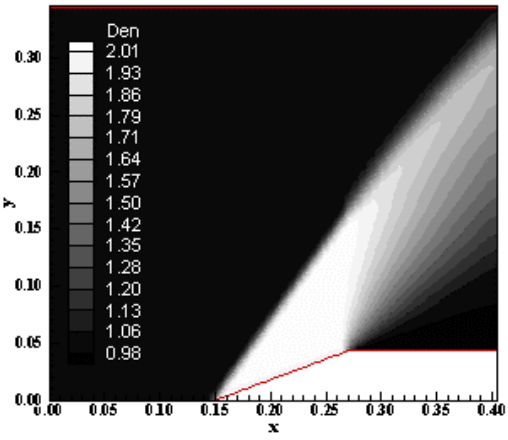

Figure 5. Density field (LS/93).

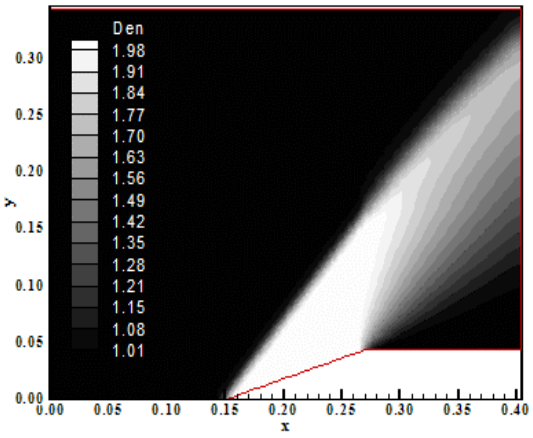

Figure 6. Density field (RK/95).

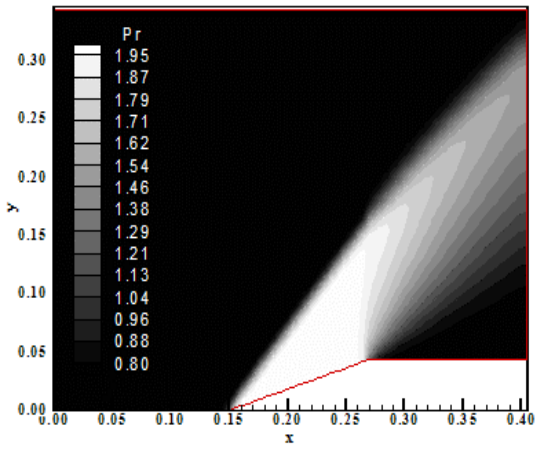

Figure 7. Pressure field (H/83).

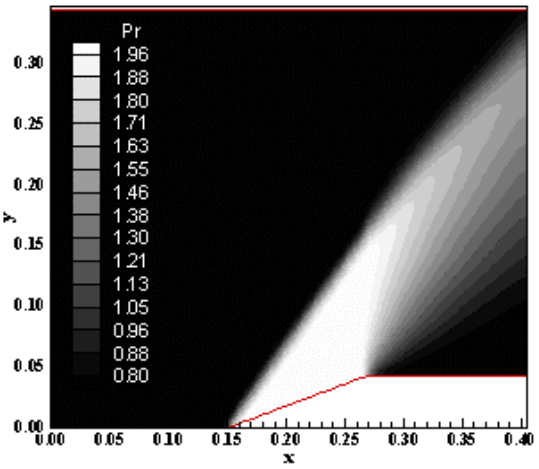

Figure 8. Pressure field (FPP/91).

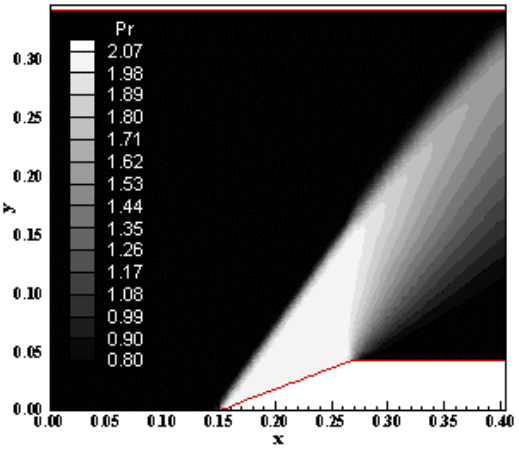

Figure 9. Pressure field (LS/93).

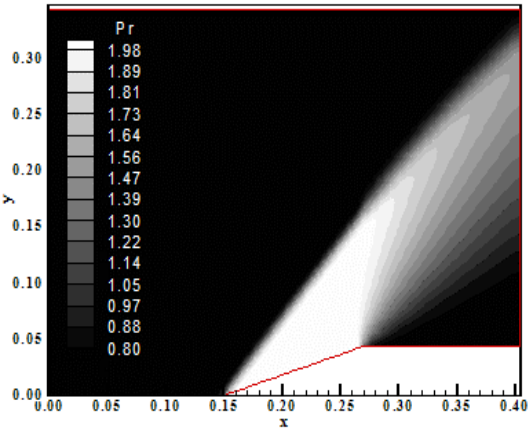

Figure 10. Pressure field (RK/95).

However, the region of maximum density (white region) generated by the Radespiel and Kroll (1995) scheme is extended in a bigger region than the other schemes.

Figures 7 to 10 exhibit the pressure fields generated by the Harten (1983), the Frink, Parikh and Pirzadeh (1991), the Liou and Steffen (1993) and the Radespiel and Kroll (1995) schemes, respectively. The pressure field generated by the Liou and Steffen (1993) scheme is the most severe in relation to the others schemes. The white region is longer in the solution generated by the Radespiel and Kroll (1995) scheme, indicating that the Radespiel and Kroll (1995) pressure solution is critical in a bigger domain region than the pressure solutions of the other schemes.

Figures 11 to 14 show the solutions obtained by the Harten (1983), the Frink, Parikh and Pirzadeh (1991), the Liou and Steffen (1993) and the Radespiel and Kroll (1995) algorithms to the Mach number field. The Mach number field generated by the Radespiel and Kroll (1995) scheme is the most intense in relation to the other schemes.

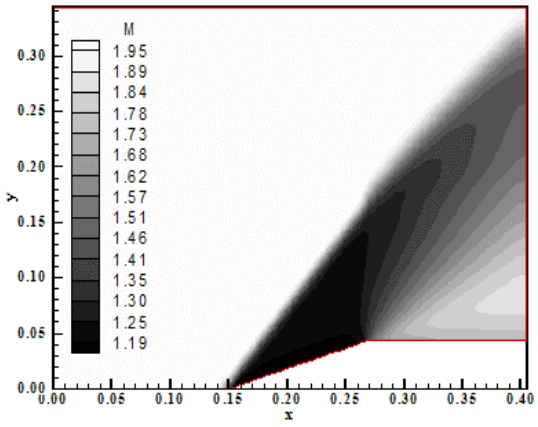

Figure 11. Mach number field (H/83).

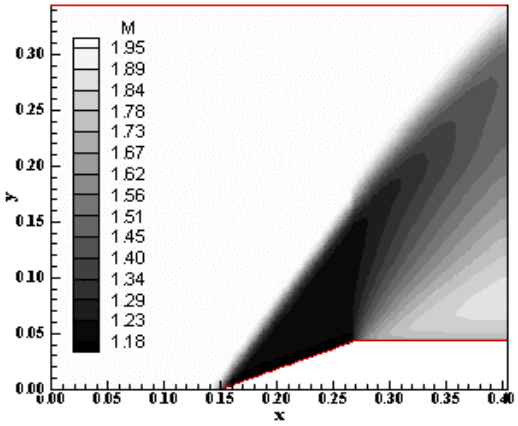

Figure 12. Mach number field (FPP/91).

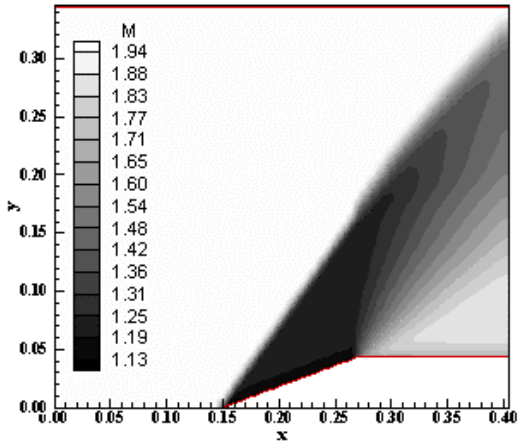

Figure 13. Mach number field (LS/93).

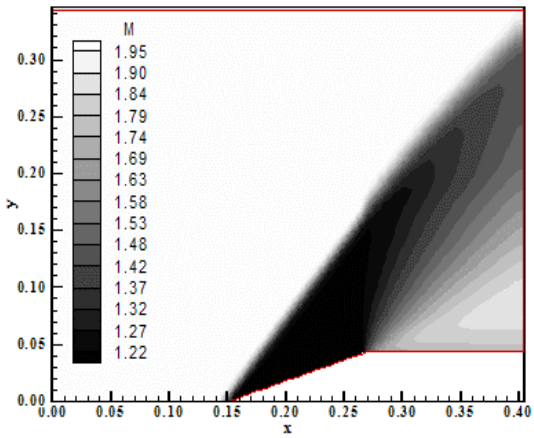

Figure 14. Mach number field (RK/95).

Figure 15 exhibits the wall pressure distribution obtained by the Harten (1983), the Frink, Parikh and Pirzadeh (1991), the Liou and Steffen (1993) and the Radespiel and Kroll (1995) schemes. They are compared with the oblique shock wave and Prandtl-Meyer expansion wave theories. As can be observed, the Harten (1983) solution presents the best pressure distribution in relation to the other solutions.

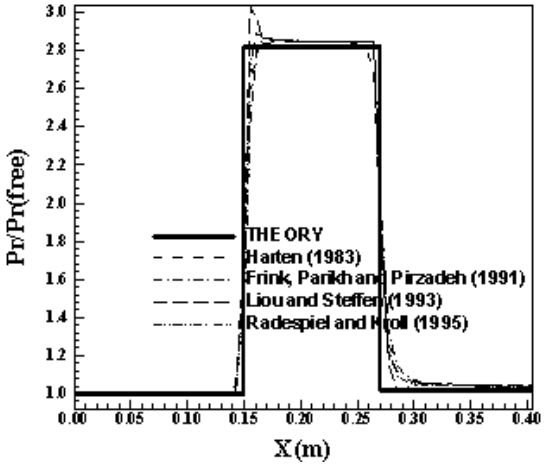

Figure 15. Wall pressure distributions.

Moreover, in the solutions generated by the Frink, Parikh and Pirzadeh (1991) and the Radespiel and Kroll (1995) schemes, there is a small pressure peak in the shock region which constitutes an error. The shock detected by the Liou and Steffen (1993) scheme presents a pressure peak which is 5.6% bigger than the maximum pressure value obtained by the Harten (1983) scheme. On the other hand, the Harten (1983) pressure solution is well defined in the constant pressure region, without any peak. The expansion fan is well characterized in all solutions, except in the Liou and Steffen (1993) solution, where it seems an expansion shock, due to its more linear behavior at the ramp end.

It is possible to conclude to this example that the Liou and Steffen (1993) scheme has presented the most critical solutions than the others schemes, although the pressure distribution along the ramp obtained by the Harten (1983) solution is the best one.

Blunt Body Physical Problem

An algebraic mesh of 103x100 points was used, which is composed of 10,098 rectangular cells and 10,300 nodes, on a finite volume context. The far field was positioned at 20.0 times the blunt body's nose curvature ratio. Figures 16 and 17 show the blunt body configuration and the employed mesh. The initial condition adopted a freestream Mach number equals to 5.0; however, the Frink, Parikh and Pirzadeh (1991) scheme only simulated this problem with a freestream Mach number equals to 2.0. Both initial conditions characterize supersonic flows.

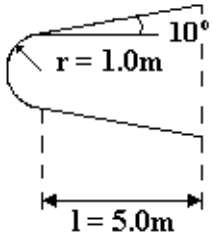

Figure 16. Blunt body configuration.

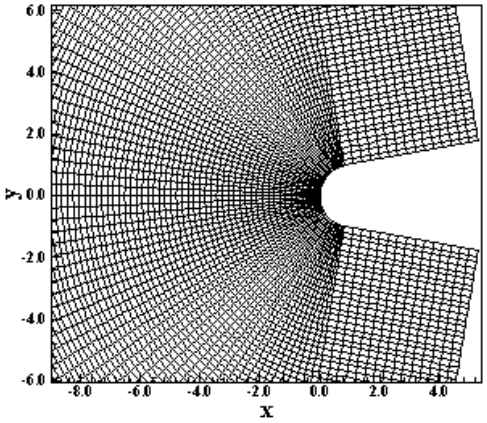

Figure 17. Blunt body mesh.

Figures 18 to 21 exhibit the density field obtained by the Harten (1983), the Frink, Parikh and Pirzadeh (1991), the Liou and Steffen (1993) and the Radespiel and Kroll (1995) schemes, respectively. The density field generated by the Liou and Steffen (1993) scheme is the densest in relation to the other schemes. The density field generated by the Frink, Parikh and Pirzadeh (1991) scheme is the lowest one in relation to the solutions of the other schemes because it simulates a less critical initial condition.

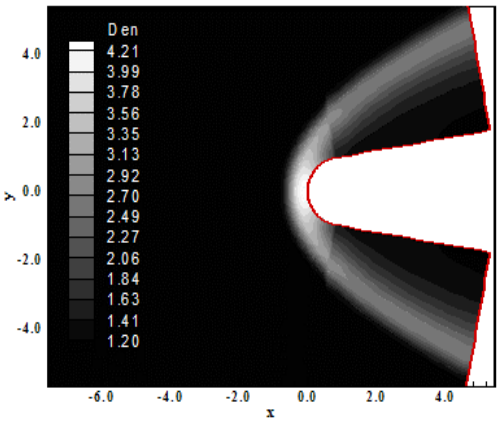

Figure 18. Density field (H/83).

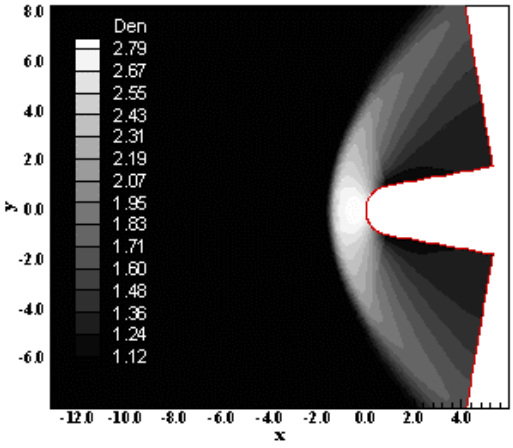

Figure 19. Density field (FPP/91).

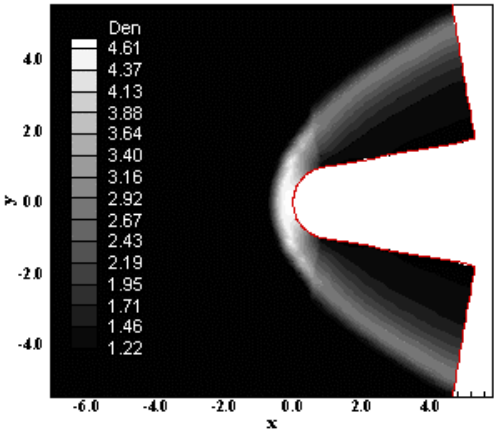

Figure 20. Density field (LS/93)

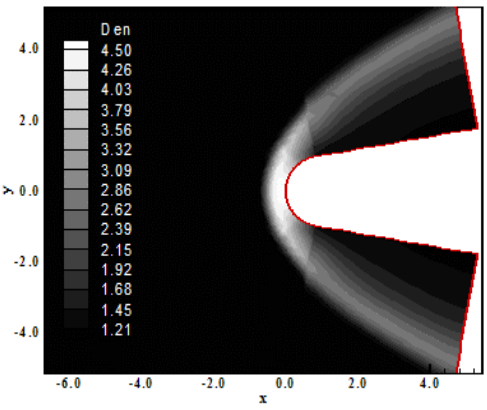

Figure 21. Density field (RK/93).

Figures 22 to 25 show the pressure fields generated by the Harten (1983), the Frink, Parikh and Pirzadeh (1991), the Liou and Steffen (1993) and the Radespiel and Kroll (1995) schemes, respectively. The pressure field generated by the Liou and Steffen (1993) scheme is again the most strength in relation to the others schemes. It is interesting to note that the Liou and Steffen (1993) scheme simulated a pressure peak approximately 434% more severe than the pressure peak simulated by the Frink, Parikh and Pirzadeh (1991) scheme. So, the Liou and Steffen (1993) scheme can support a critical pressure peak 434% more severe than the Frink, Parikh and Pirzadeh (1991) scheme can support.

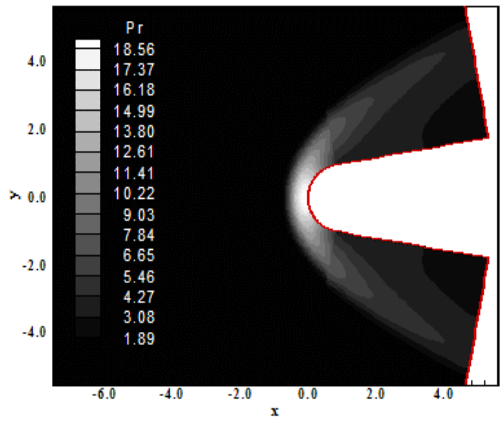

Figure 22. Pressure field (H/83).

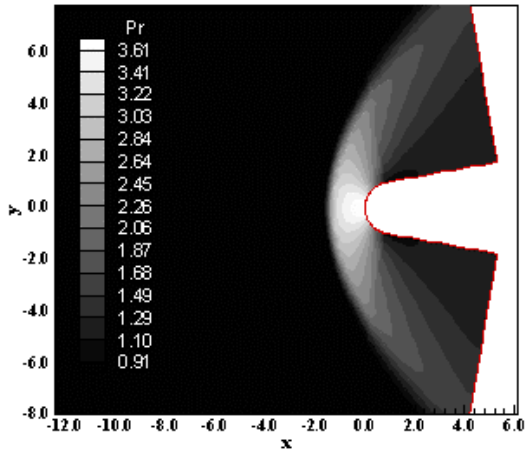

Figure 23. Pressure field (FPP/91).

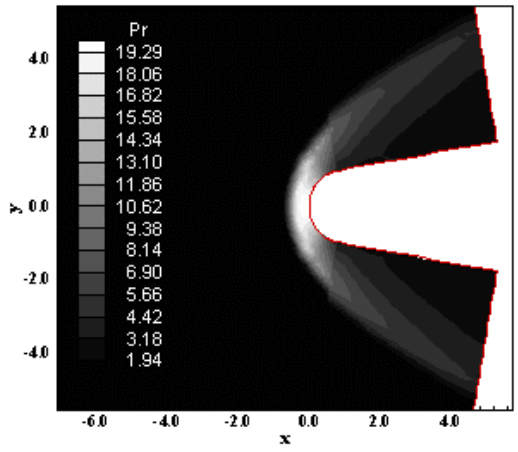

Figure 24. Pressure field (LS/93).

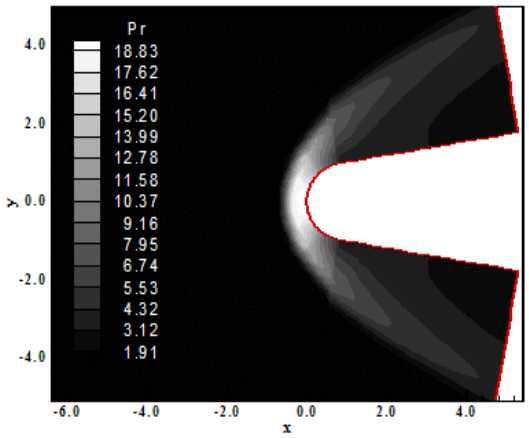

Figure 25. Pressure field (RK/95).

Figures 26 to 29 exhibit the Mach number fields generated by the Harten (1983), the Frink, Parikh and Pirzadeh (1991), the Liou and Steffen (1993) and the Radespiel and Kroll (1995) algorithms, respectively. The Mach number field generated by the Harten (1983) and by the Liou and Steffen (1993) schemes are more intense than those generated by the Frink, Parikh and Pirzadeh (1991) and the Radespiel and Kroll (1995) schemes.

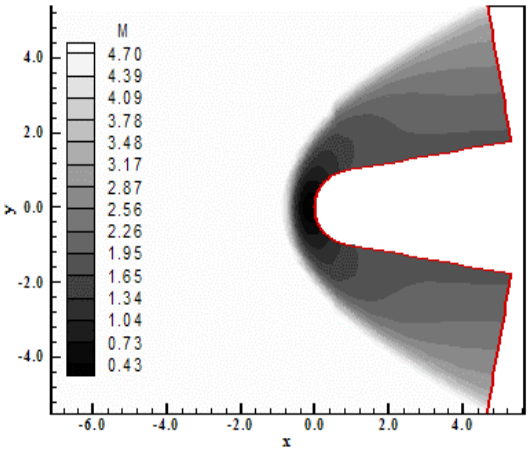

Figure 26. Mach number field (H/83).

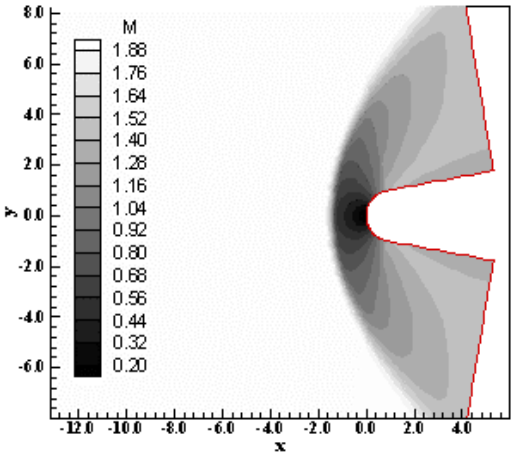

Figure 27. Mach number field (FPP/91).

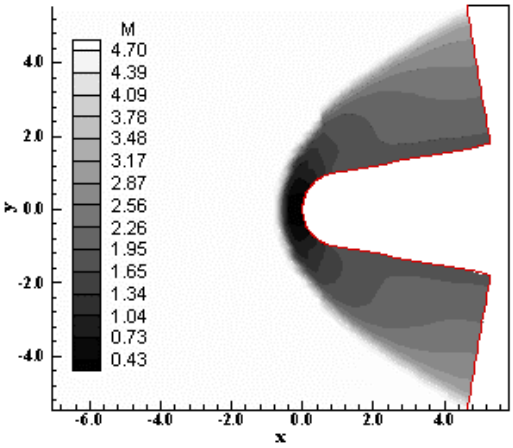

Figure 28. Mach number field (LS/93).

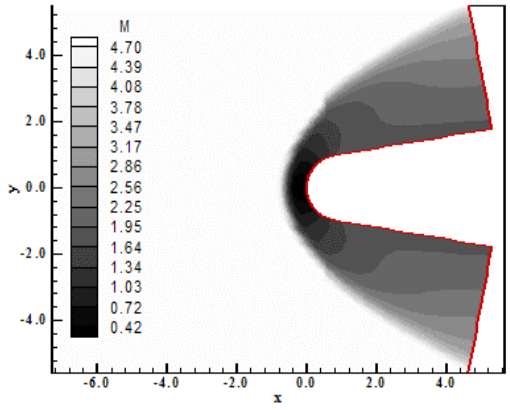

Figure 29. Mach number field (RK/95).

Figure 30 presents the -Cp distributions generated by the Harten (1983), the Frink, Parikh and Pirzadeh (1991), the Liou and Steffen (1993) and the Radespiel and Kroll (1995) schemes. The Liou and Steffen (1993) solution presents the biggest value of Cp at the configuration nose in relation to the solutions of the other schemes. It is possible to note that the Liou and Steffen (1993) solution detects a Cp peak of 1.58, while the Cp peak obtained by the Harten (1983) solution, the lowest value of Cp, is equals to 1.52, which represents a difference of about 4.0% in relation to Harten (1983) solution.

The aerodynamic coefficients of lift and drag to this problem for each scheme are shown in Tab. 2. The zero values exhibited in this table are accurate until fourteen digits after the comma. It is possible to conclude that to this symmetrical blunt body configuration and to a zero attack angle, the value of c_L equals to zero correspond to the expected solution. Hence, this coefficient was well calculated by all schemes, except the Harten (1983) scheme.

Table 2. Aerodynamic coefficients of lift and drag.

Algorithm	c_L	c_D
Harten (1983)	-1.054×10^{-4}	-8.982×10^{-6}
Frink, Parikh and Pirzadeh (1991)	0.0	0.0
Liou and Steffen (1993)	0.0	0.0
Radespiel and Kroll (1995)	0.0	0.0

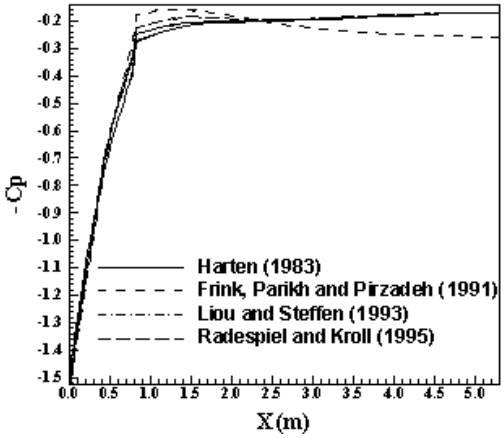

Figure 30. -Cp distributions.

Another possibility to quantitative comparison of the schemes is the determination of the stagnation pressure ahead of the configuration. Anderson (1984) presents a table of normal shock wave properties in its B Appendix. This table permits the determination of some shock wave properties as function of the freestream Mach number. In front of the blunt body configuration studied in this work, the shock wave presents a normal shock behavior, which permits the determination of the stagnation pressure, behind the shock wave, from the tables encountered in Anderson (1984). So it is possible to determine the ratio pr_0 / pr_∞ from Anderson (1984), where pr_0 is the stagnation pressure in front of the configuration and pr_∞ is the freestream pressure (equals to $1/\gamma$ to the present nondimensionalization).

Hence, to this problem, $M_\infty = 5.0$ corresponds to $pr_0 / pr_\infty = 32.65$ and remembering that $pr_\infty = 0.714$, it is possible to conclude that $pr_0 = 23.31$. Table 3 presents the stagnation pressure obtained by each scheme and the respective percentage errors. The Liou and Steffen (1993) scheme presents the best solution.

Table 3. Stagnation pressure and percentage errors.

Algorithm	pr_0	Error (%)
Harten (1983)	18.56	25.6
Liou and Steffen (1993)	19.29	20.8
Radespiel and Kroll (1995)	18.83	23.8

It is possible to conclude that the Liou and Steffen (1993) scheme, a flux vector splitting scheme, presents the most critical solutions, in both example-cases, in relation to the other schemes and a more accurate solution, in terms of the determination of the stagnation pressure in the blunt body case, than the Harten (1983) and the Radespiel and Kroll (1995) schemes.

Numerical Data of the Simulations and Computational Costs

Table 4 exhibits the numerical data of the simulations with the respective computational cost of the algorithms. The most expensive scheme is the Frink, Parikh and Pirzadeh (1991) one, being 4,641% more expensive than the Liou and Steffen (1993) scheme, the cheapest.

Table 4. Numerical data of the simulations and computational costs.

	Ramp		Blunt Body		
Algorithm	CFL	Iterations	CFL	Iterations	Cost(1)
Harten (1983)	0.9	996	0.9	757	0.0000301
Frink, Parikh and Pirzadeh (1991)	1.6	548	1.2	1,001(2)	0.0001612
Liou and Steffen (1993)	0.9	1,021	0.9	1,168	0.0000034
Radespiel and Kroll (1995)	0.9	996	0.9	1,049	0.0000258

(1): Measured in seconds/per cell/per iteration.
(2): The scheme simulated this problem with less severe initial conditions.

Conclusions

The present work aimed a comparative study among the structured upwind schemes of Harten (1983), of Frink, Parikh and Pirzadeh (1991), of Liou and Steffen (1993) and of Radespiel and Kroll (1995), applied to aeronautical and aerospace problems. The schemes are first order accurate in space, being the Harten (1983) scheme a TVD flux difference splitting method, the Frink, Parikh and Pirzadeh (1991) scheme a flux difference splitting method, the Liou and Steffen (1993) and the Radespiel and Kroll (1995) schemes flux vector splitting methods. All schemes were applied to the solution of the physical problems of the supersonic flows along a ramp and around a blunt body configuration, with zero attack angle. All algorithms are accelerated to the steady state solution using a spatially variable time step. This technique has proved excellent gains in terms of convergence ratio as reported in Maciel (2005).

The results have demonstrated that the Liou and Steffen (1993) scheme has presented the most critical solutions, in both example-cases, in relation to the other schemes and a more accurate solution, in terms of the determination of the stagnation pressure in blunt body case, than the Harten (1983) and the Radespiel and Kroll (1995) schemes. The Harten (1983) scheme has presented the best pressure distribution along the ramp wall in relation to the other schemes. In the blunt body problem, the Liou and Steffen (1993) scheme presents the highest value of Cp at the configuration nose in relation to the others schemes. Values of c_L and c_D have been accurately predicted by all schemes, except by the Harten (1983) scheme. The Liou and Steffen (1993) scheme predicts the most accurate value of the stagnation pressure in front of the configuration in relation to the other schemes. In terms of computational cost, the cheapest scheme is the Liou and Steffen (1993) scheme, being about 4,641% less expensive than the Frink, Parikh and Pirzadeh (1991) scheme, the most expensive.

More studies, with other example-cases, will be performed by this author aiming to better detect the characteristics of the algorithms presented in this work.

References

Anderson, J. D., 1984, "Fundamentals of Aerodynamics", McGraw-Hill, Inc., EUA, 563p.

Frink, N. T., Parikh, P., and Pirzadeh, S., 1991, "Aerodynamic Analysis of Complex Configurations Using Unstructured Grids", AIAA 91-3292-CP.

Harten, A., 1983, "High resolution schemes for hyperbolic conservation laws", *Journal of Computational Physics*, Vol. 49, pp. 357-393.

Jameson, A. and Mavriplis, D. J., 1986, "Finite volume solution of the two-dimensional Euler equations on a regular triangular mesh", *AIAA Journal*, Vol. 24, No. 4, pp. 611-618.

Kutler, P., 1975, "Computation of three-dimensional, inviscid supersonic flows", *Lecture Notes in Physics*, Vol. 41, pp. 287-374.

Liou, M., and Steffen, C. J., Jr., 1993, "A new flux splitting scheme", *Journal of Computational Physics*, Vol. 107, pp. 23-39.

Maciel, E. S. G., 2002, "Simulação numérica de escoamentos supersônicos e hipersônicos utilizando técnicas de dinâmica dos fluidos computacional", Doctoral thesis, ITA, CTA, São José dos Campos, SP, Brazil, 258 p.

Maciel, E. S. G., 2005, "Analysis of convergence acceleration techniques used in unstructured algorithms in the solution of aeronautical problems – part I", Proceedings of the XVIII COBEM International Congress of Mechanical Engineering, Ouro Preto, MG, Brazil.

Maciel, E. S. G., 2006, "Comparison between the Yee, Warming and Harten and the Hughson and Beran high resolution algorithms in the solution of the Euler equations in two-dimensions – theory", Proceedings of the XXVII CILAMCE Iberian Latin-American Congress on Computational Methods in Engineering, Belém, PA, Brazil.

Maciel, E. S. G., 2007, "Solutions of the Euler and the Navier-Stokes equations using the Jameson and Mavriplis and the Liou Steffen unstructured algorithms in three-dimensions", *Journal of Engineering Applications of Computational Fluid Mechanics*, China, Vol. 1, No. 4, pp. 238-252.

Radespiel, R., and Kroll, N., 1995, "Accurate flux vector splitting for shocks and shear layers", *Journal of Computational Physics*, Vol. 121, pp. 66-78.

Roe, P. L., 1981, "Approximate Riemann solvers, parameter vectors, and difference schemes", *Journal of Computational Physics*, Vol. 43, pp. 357-372.

Steger, J. L., 1978, "Implicit finite-difference simulation of flow about arbitrary two-dimensional geometries", *AIAA Journal*, Vol. 16, No. 7, pp. 679-686.

Van Leer, B., 1982, "Flux-vector splitting for the Euler equations", Proceedings of the 8th International Conference on Numerical Methods in Fluid Dynamics, E. Krause, Editor, *Lecture Notes in Physics*, Vol. 70, pp. 507-512, Springer-Verlag, Berlin.